Radial displacement of a fluid annulus in a rotating Hele–Shaw cell

Lluís Carrillo, Jordi Soriano, and Jordi Ortín

Citation: Physics of Fluids (1994-present) **11**, 778 (1999); doi: 10.1063/1.869950

View online: http://dx.doi.org/10.1063/1.869950

View Table of Contents: http://scitation.aip.org/content/aip/journal/pof2/11/4?ver=pdfcov

Published by the AIP Publishing

Radial displacement of a fluid annulus in a rotating Hele–Shaw cell

Lluís Carrillo, Jordi Soriano, and Jordi Ortín
Departament d'Estructura i Constituents de la Matèria, Facultat de Física, Universitat de Barcelona, Diagonal 647, E-08028 Barcelona, Catalonia, Spain

(Received 8 May 1998; accepted 30 November 1998)

The radial displacement of a fluid annulus in a rotating circular Hele–Shaw cell has been investigated experimentally. It has been found that the flow depends sensitively on the wetting conditions at the outer interface. Displacements in a prewet cell are well described by Darcy's law in a wide range of experimental parameters, with little influence of capillary effects. In a dry cell, however, a more careful analysis of the interface motion is required; the interplay between a gradual loss of fluid at the inner interface, and the dependence of capillary forces at the outer interface on interfacial velocity and dynamic contact angle, result in a constant velocity for the interfaces. The experimental results in this case correlate in the form of an empirical scaling relation between the capillary number Ca and a dimensionless group, related to the ratio of centrifugal to capillary forces, which spans about three orders of magnitude in both quantities. Finally, the relative thickness of the coating film left by the inner interface, α_i, is obtained as a function of Ca. © *1999 American Institute of Physics.* [S1070-6631(99)02503-9]

I. INTRODUCTION

The study of fluid flows in the narrow gap between two parallel plates (Hele–Shaw cell) has been a subject of sustained interest since the pioneering work of Saffman and Taylor.[1] The simplicity of the equations describing the flow, which lead to Darcy's law, in contrast with the rich phenomenology observed, has stimulated the interest of researchers in exploring the problem both theoretically and experimentally.[2,3] Most of the situations studied correspond to the evolution of an interface between two fluids of different viscosity and/or different density, in the presence of a pressure field.

In both the channel and the circular (axisymmetric) geometry, most efforts have focused on the case where the less viscous fluid displaces the more viscous one.[4–8] In particular, all the theoretical efforts to prescribe appropriate boundary conditions at the interface have considered the less viscous fluid as the invader.[9]

In the opposite scenario, studied here, a more viscous fluid displaces a less viscous fluid, and the interfacial instability is driven by the density contrast between the two fluids in the presence of gravity[1,10] or a centrifugal force.[11,12] Related to this problem, Elliot and Riddiford[13] studied the dynamic contact angle θ_D when oil displaces air in the circular geometry. Cardoso and Woods[14] focused their attention on the problem of a fluid annulus confined between two other fluids of different viscosity and displaced by the inner fluid. In this configuration one interface of the annulus may become unstable, and the interplay between the two interfaces gives rise to a new phenomenology. A similar situation can be established if a fluid annulus is rotated around its vertical axis in a circular Hele–Shaw cell. Modifying the different adjustable parameters of the experiment, a variety of phenomena can be explored depending on whether none of the two interfaces, one of them or both become unstable. This kind of investigation was suggested by Melo *et al.*[15] in their work on the evolution of rotating drops, extended to viscoelastic fluids by Spaid and Homsy[16] some years later.

Before pursuing a study of the instability, however, it is important to achieve a thorough understanding of the regime for which the annulus evolves in a stable manner. This regime turns out to be interesting by itself, because the evolution of the circular annulus does not follow from the Hele–Shaw equations in a trivial way. Basically, there are two new aspects to consider (i) the formation of a fluid film behind the inner interface as the annulus moves radially, which may result in a gradual mass loss, and (ii) the wetting conditions encountered by the advancing outer interface, particularly the influence of the front velocity on the contact angle.[13,17,18] Although these ingredients make the problem rather complex from a theoretical point of view, we have found that experimental observations can be collapsed in a robust and relatively simple way, which provide a firm basis for a rigorous theoretical approach. Consequently, we have chosen to restrict the present paper to the study of the radial displacement of the rotating annulus in the stable regime, and leave for a second paper[19] our results on the linear and nonlinear regimes of the fingering instability experienced by the two interfaces of the annulus.

The outline of the work is the following: Sec. II presents a description of the experiment, a discussion of the necessary conditions for the formation of the fluid annulus in a rotating Hele–Shaw cell, the equations for the flow in the Hele–Shaw approximation, and their solution for the velocity field in the bulk of the liquid phase. In Sec. III we describe the experimental procedure, study the influence of wetting on the flow through the boundary conditions, and present the experimental results. The results are discussed in Sec. IV, and the conclusions given in Sec. V.

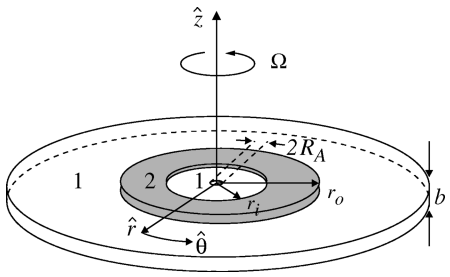

FIG. 1. Sketch of the circular Hele–Shaw cell, and the notation used.

II. RADIAL DISPLACEMENT OF A ROTATING FLUID ANNULUS

A. Description of the experiment

The Hele–Shaw cell used in the present investigation is made of two circular glass plates of thickness 6 mm and radius 200 mm, placed on top of each other, separated a distance b by means of appropriate spacers located on the edge of the cell, which is open to air (Fig. 1). The cell is placed on a sturdy rotating platform driven by a dc motor and reductor. Details of both the experimental setup and the image acquisition system can be found in Ref. 12. The fluids used are (i) a silicone oil (Rhodorsil 47 V) of kinematic viscosity $\nu=50$ or 500 mm^2/s, density $\rho=998$ kg/m^3, and surface tension $\sigma=20.7$ mN/m at 25 °C, and (ii) a vaseline oil of $\nu=150$ mm^2/s, $\rho=870$ kg/m^3, and $\sigma=29.3$ mN/m at 25 °C. The kinematic viscosity ν is related to the dynamic viscosity μ by $\nu=\mu/\rho$. The oils wet the glass plates well. They are injected into the cell by means of a syringe pump through a central orifice of radius $R_A=4$ mm machined in the upper plate. As the liquid enters the cell, a circular drop forms in the narrow gap between the two plates and is let to grow up to a prescribed radius L. At this stage injection ends, and the cell is set to rotate with angular velocity Ω. Both interfaces move outwards due to centrifugal forces.

B. Conditions for the formation of the fluid annulus

A first question to consider is the possibility of forming a fluid annulus from a circular drop placed at the center of a rotating cell. The conditions for an initially compact fluid drop to shrink along the vertical direction, at the center of the drop, and break up to form a fluid annulus, are the following. The pressure applied on the liquid surface at the central orifice of the upper plate must be large enough to bend the surface until it touches the lower plate. In these conditions, the curvature of the central part of the drop will be $\kappa_{R_A}=2b/(b^2+R_A^2)$ provided $R_A>b$. The pressure required to achieve this curvature is $p_{R_A}\simeq\sigma\kappa_{R_A}$. Since the pressure due to inertial forces when the cell rotates around its central axis is given by $p_\Omega\simeq\frac{1}{2}\rho\Omega^2L^2$, the condition $p_\Omega>p_{R_A}$ for breaking up the liquid results in

$$\frac{1}{2}\rho\Omega^2L^2>\frac{2b\sigma}{b^2+R_A^2}. \tag{1}$$

Once formed, the condition for the annulus to move outwards is

$$\frac{1}{2}\rho\Omega^2L^2>\sigma\left(\frac{1}{R_A}+\frac{1}{L}\right), \tag{2}$$

because there is no viscous pressure (the initial velocity of the interfaces is zero) and the only pressure difference is due to capillarity. Since $R_A\ll L$, satisfying Eq. (2) implies satisfying Eq. (1) as well. For a drop of initial radius $L=30$ mm and $\nu=50$ mm^2/s the threshold given by Eq. (2) is $\Omega\simeq30$ rev/min, in good agreement with our observations.

C. Modeling

In the Hele–Shaw approximation the velocity field in the bulk of the fluid, averaged in the direction perpendicular to the plates, obeys Darcy's law,

$$\mathbf{v}_j=\nabla\phi_j, \tag{3}$$

where

$$\phi_j=-\frac{b^2}{12\mu_j}\left(p_j-\frac{1}{2}\rho_j\Omega^2r^2\right), \tag{4}$$

when the fluid rotates with angular velocity Ω, and j indexes the two fluids (1: air, 2: oil). For an incompressible fluid, Darcy's law takes the form

$$\Delta\phi_j=0. \tag{5}$$

The validity of the Hele–Shaw approximation in our problem is justified by the small values of Reynolds and Rossby number, $\mathrm{Re}=U_rb^2/\nu L<0.02$ and $Rs=U_r/\Omega L<0.03$. Here, U_r represents a typical radial velocity in the problem.

Boundary conditions are first stablished by the pressure jump at the two interfaces;

$$\begin{aligned}(p_1-p_2)_i&=\sigma(\kappa_{\perp i}+\kappa_{\parallel i}),\\(p_1-p_2)_o&=\sigma(\kappa_{\perp o}-\kappa_{\parallel o}),\end{aligned} \tag{6}$$

where the index i refers to the inner interface and the index o to the outer interface. $\kappa_\perp$ and $\kappa_\parallel$ are the curvatures of the interface in the directions perpendicular and parallel to the plates, respectively. The curvatures are given by

$$\begin{aligned}\kappa_{\perp i}&=\frac{2}{b}\gamma_{\perp i},\quad \kappa_{\parallel i}=\frac{1}{r_i}\gamma_{\parallel i},\\\kappa_{\perp o}&=\frac{2}{b}\gamma_{\perp o},\quad \kappa_{\parallel o}=\frac{1}{r_o}\gamma_{\parallel o},\end{aligned} \tag{7}$$

where the dimensionless coefficients γ account for possible influences of the coating film left behind the inner interface and variations of the contact angle of the advancing outer interface.

The continuity of the normal velocity across the two interfaces leads to a second set of boundary conditions (see Fig. 2),

$$\partial_r\phi_1|_i=\partial_r\phi_2|_i\ \frac{1}{1-\alpha_i},\quad \partial_r\phi_1|_o=\partial_r\phi_2|_o\ \frac{1}{1-\alpha_o}. \tag{8}$$

The first one expresses the condition that, at the inner interface, the normal velocity of the air meniscus is larger than the velocity in the bulk of the liquid predicted by Laplace's equation by a factor $1/(1-\alpha_i)$. This effect is due to the two

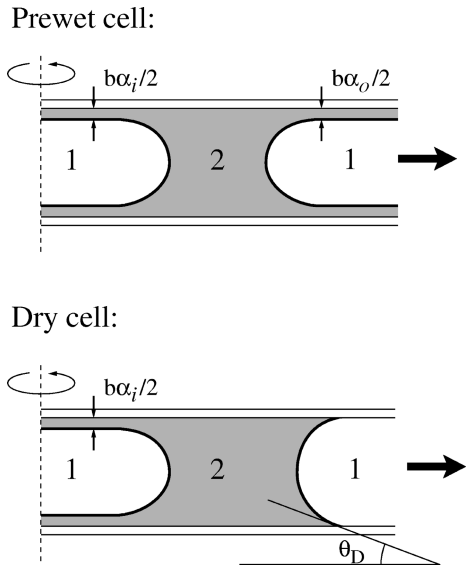

FIG. 2. Sketch of the meniscii at the inner and outer interfaces of the fluid annulus, moving in a prewet cell and in a dry cell.

coating films (one on each plate) left behind the inner interface, of thickness $b\alpha_i/2$.[20,21] Actually, the form adopted for this term is valid for a coating film at rest. When the motion of the coating film is taken into account there are corrective terms of the order $(\alpha_i/2)^2$ to be considered, and the density of the fluid in the potential ϕ_2 must be replaced by an effective density $\rho_2^*=(1-B)\rho_2$, where $B\sim(\alpha_i/2)^3$.[1] In the limit $\alpha_i \ll 1$, however, these corrections are negligible. The second equation in (8) expresses an equivalent condition for the outer interface, which may either absorb fluid from two wetting films of thickness $b\alpha_o/2$ (if the plates have been prewetted before the experiment, as explained in Sec. III), or move in a dry cell ($\alpha_o=0$).

The last condition to consider is the conservation of the total mass of liquid during the displacement of the annulus. The mass of liquid in the annulus is given instantaneously by $\rho\pi bL^2(t)=\rho\pi b(r_o^2-r_i^2)$. Therefore, the fluid mass in the annulus changes in time according to $\partial_t L^2=2r_o v_o-2r_i v_i=2r_o\partial_r\phi_1|_o-2r_i\partial_r\phi_1|_i$. Using the boundary conditions given in Eq. (8), and the fact that in the bulk of the liquid the solution of Laplace's equation (5) leads to $v\sim 1/r$ for $r_i<r<r_o$, we get

$$\partial_t L^2=-2r_i\partial_r\phi_1|_i\frac{\alpha_i-\alpha_o}{1-\alpha_o}. \tag{9}$$

Since $\partial_r\phi_1|_i=\partial_t r_i$, the solution of the differential equation for $L^2(t)$ reads

$$L^2(t)=L^2(0)-\frac{\alpha_i-\alpha_o}{1-\alpha_o}r_i^2(t). \tag{10}$$

This result shows that the mass of liquid in the annulus is conserved only if $\alpha_i=\alpha_o$, i.e., if the thickness of the wetting films is the same at both inner and outer interface. If $\alpha_i>\alpha_o$, the amount of liquid between the two interfaces decreases with time.

To derive the radial velocity of the flow in the bulk of the liquid, notice that the velocity potential of the axisymmetric problem given by Eq. (5), expressed in planar polar coordinates, is

$$\phi_j(r)=A_j\ln r+B_j. \tag{11}$$

Using Eq. (3), the radial velocity field (averaged along z) is given by

$$v_j(r)=\frac{A_j}{r}. \tag{12}$$

The boundary conditions (6) can be used to determine the constants A_j in Eq. (12). The potential ϕ can be considered constant for air. Dropping then the subscripts, because all the parameters refer now to fluid 2, we get for the velocity field in r,

$$v(r;t)=\frac{b^2}{12\mu}\frac{\frac{1}{2}\rho\Omega^2L^2(t)-\sigma[\kappa_{\perp i}-\kappa_{\perp o}+\kappa_{\parallel i}+\kappa_{\parallel o}]}{\frac{r}{2}\ln\left[\frac{L^2(t)}{r_i^2}+1\right]}, \tag{13}$$

where the condition $L^2(t)=r_o^2-r_i^2$ has been used in the denominator.

III. EXPERIMENTAL PROCEDURE AND RESULTS

We have performed experiments with gap spacings $b=0.25$, 0.50, 0.81, 1.00, 1.94, and 2.94 (± 0.05) mm, angular velocities $\Omega_0=30$, 60, 90, 120, 150, 180, 210, 240, 270, and 300 rev/min, and initial radii $L(0)$ between 15 and 120 mm.

Special care has been taken in cleaning the Hele–Shaw cell before starting a new experiment. Oil traces have been removed using blotting paper. The plates have been thoroughly cleaned with soap and water, rinsed with distilled water and acetone, and finally dried with a jet of pressurized air. The cleaning is performed in random circles to avoid any preferential wetting direction on the plates.

The experiments can be classified into two large classes, depending on the wetting properties of the plates resulting from two different initial preparations. In the first class, the two inner surfaces of the cell plates are previously wetted with a thin oil layer in the following way: oil is slowly injected into the motionless cell, up to a radius of about 100 mm; next, the turning platform is switched on at low speed (between 40 and 60 rev/min), and the oil bubble spreads in the form of an annulus, which grows until the inner circular interface leaves the cell at the open boundary. In this way, the cell is prewetted with a thin oil layer on each plate. To avoid the subsequent formation of oil drops on the plates, a new fluid annulus is formed immediately by additional oil injection, and the experiment is started. In the second class of experiments, the plates are left dry. Figure 3 shows the different evolutions of the two fluid annulus prepared in identical experimental conditions, one in a prewet cell and the other in a dry cell.

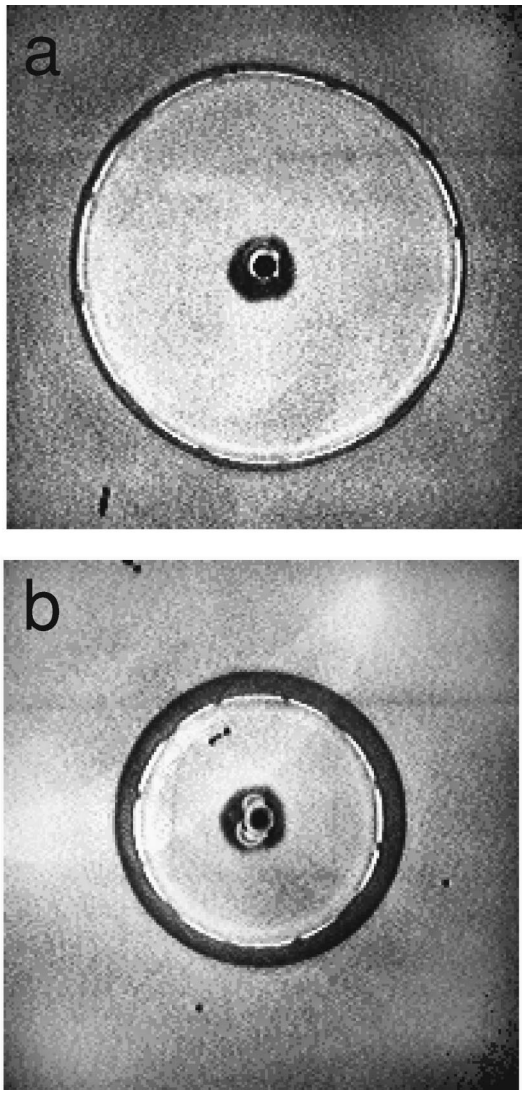

FIG. 3. Evolution of two fluid annulus in identical experimental conditions ($b=0.81$ mm, $L=30$ mm, and $\Omega=150$ rev/min), advancing in a prewet cell (a) and in a dry cell (b). Both images have been recorded 8 s after the cell started rotating.

A. Displacement in a prewet cell

When the displacement takes place in a prewet cell, two approximations can be reasonably made. The first approximation is neglecting capillary forces in front of inertial forces. There are two reasons for this: (i) dynamic contact angles at both interfaces are close to zero (full wetting) and therefore the term $\kappa_{\perp i}-\kappa_{\perp o}$, which behaves as $(2/b)\times(\cos\theta_{Di}-\cos\theta_{Do})$, is very close to zero; (ii) the term $\kappa_{\parallel i}-\kappa_{\parallel o}$ behaves as $1/r$, and hence it is also close to zero practically from the formation of the drop. Notice that we neglect the *net* contribution of capillary forces when the two interfaces are considered at the same time, but capillary forces at each individual interface are responsible for their stability. The second approximation is to consider $L^2(t)$ constant, at least for a large fraction of the experiment. The reason now is that in a prewet cell the mass transferred to the oil film left behind the inner interface of the advancing annulus is balanced to some extent by the mass gained from the wetting layer by the outer interface (Fig. 2). Our measurements show that the loss of fluid in the annulus in the early and intermediate stages of the run is negligible, and only at the end increases to about 10% maximum.

With these approximations in mind, the velocity in the fluid phase at the inner interface, derived from Eq. (13), reads

$$v(r_i)=\frac{b^2}{12\mu}\frac{\frac{1}{2}\rho\Omega^2L^2}{\frac{r_i}{2}\ln\left(\frac{L^2}{r_i^2}+1\right)}. \tag{14}$$

At this point, we take the additional approximation that in the prewet cell the velocity v_i of the inner interface is well approximated by $v(r_i)$. Actually, according to Eq. (8), v_i is larger than $v(r_i)$ by a factor $1/(1-\alpha_i)$, where α_i, on its turn, depends on $v(r_i)$. Our results will show that this correcting factor is very close to one, except for the latest stages of the runs where the other approximations fail as well.

With this additional approximation, we can integrate Eq. (14) between $t=0$ and t, assuming that Ω reaches the steady value Ω_0 instantaneously at $t=0$. We make the variables dimensionless through the changes $\tilde{r}=r/L$ and $\tilde{t}=(b^2/12\mu)\frac{1}{2}\rho\Omega_0^2t$. Since $r_i(0)=0$, we arrive at

$$(\tilde{r}_i^2+1)\ln(\tilde{r}_i^2+1)-\tilde{r}_i^2\ln\tilde{r}_i^2=\tilde{t}. \tag{15}$$

Using the approximation $a\ln(a+1)-a\ln a\simeq 1$ for $a\gg 1$, this equation reduces to $\tilde{r}_i^2=e^{\tilde{t}}-1$. The position of the outer interface is related to the position of the inner interface by the condition of mass conservation $\tilde{r}_o^2=1+\tilde{r}_i^2$.

It should be noted that, in the experiments, the turning platform cannot reach the angular velocity Ω_0 instantaneously. There is a short transient interval at the beginning of each run where Ω rises from 0 to the steady value Ω_0. The Appendix shows that the influence of this transient interval is captured by replacing t with a function $f(t)$, dependent on Ω_0, which only modifies the time axis at very short t (from 1 to 10 s) when Ω_0 is very large (from 150 to 300 rev/min).

The evolution of inner and outer radii with time in our experiments is shown in the insets of Figs. 4 and 5. Interface velocities cover a range between 9 and 40 mm/s. The result of scaling the measurements following the procedure described above is also shown in the figures. The collapse is remarkable. The measured positions of the meniscii closely follow the behavior predicted by Eq. (15), up to a dimensionless time around 0.9. At later times the theoretical line rises faster than most of the measurements.

B. Displacement in a dry cell

The evolution of inner and outer radii in a dry cell is shown in Figs. 6 and 7. While the equations describing the Hele–Shaw flow would predict a nearly exponential growth of both radii at long times (experimentally confirmed in a prewet cell), the experiments in a dry cell systematically show a linear dependence. The figures reveal that our experimental data cannot be collapsed now using the same dimensionless length and time than in Sec. III A.

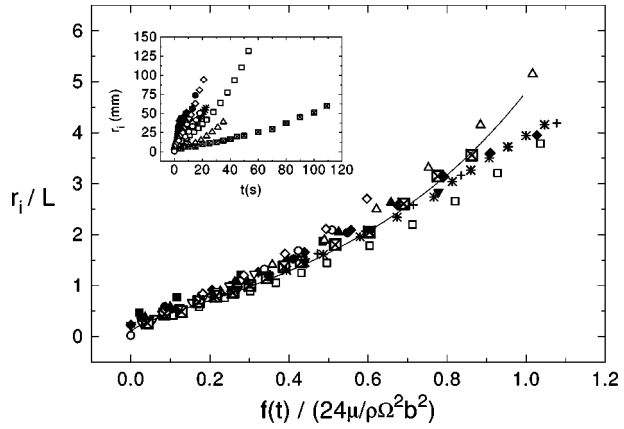

FIG. 4. Measurements of the inner radius of the fluid annulus as a function of time (corrected from initial acceleration of the cell; see Appendix), in a prewet cell under different experimental conditions. The inset shows the experimental results, and the main plot the result of scaling the measurements following the procedure explained in the text. The solid line represents Eq. (15).

Since the velocity of the inner interface remains constant in time (except for an initial transient interval in which it experiences a singularity associated with breaking the drop, very short compared to the time scale of the experiment), the capillary number $\mathrm{Ca}=\mu v_i/\sigma$ (ratio of viscous to capillary forces) turns out now to be very suitable to characterize the experiments.

In dry conditions, the mass lost by the annulus is directly related to the fluid films left behind the inner interface. Hence, a reliable estimate of α_i (the relative thickness of the two inner coating films, assumed to be constant), can be obtained from a fit of Eq. (10) with $\alpha_o=0$ (dry conditions), $L^2(t)=L^2(0)-\alpha_i r_i^2(t)$, to measurements of the surface area of the annulus as a function of inner radius. A typical result is shown in the inset of Fig. 8. The measurements of L^2 follow well the quadratic dependence on r_i expected for constant α_i. A log–log plot of the α_i obtained in this way against Ca, for the complete set of experiments with silicone oils in dry conditions, is shown in Fig. 8.

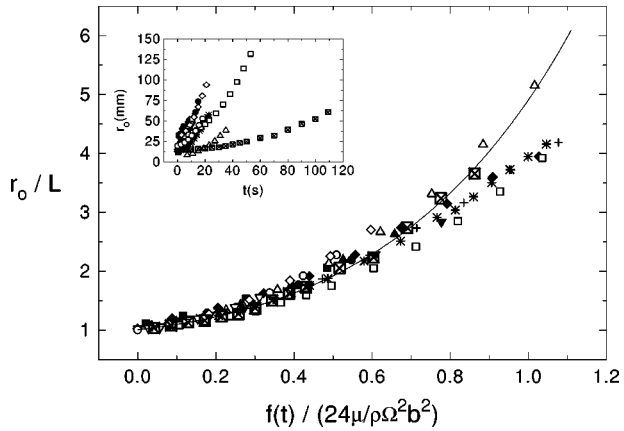

FIG. 5. Measurements of the outer radius of the fluid annulus as a function of time (corrected from initial acceleration of the cell; see Appendix), in a prewet cell under different experimental conditions. The inset shows the experimental results, and the main plot the result of scaling the measurements following the procedure explained in the text. The solid line represents r_o/L, obtained from Eq. (15) and the condition of mass conservation $\tilde{r}_o^2=1+\tilde{r}_i^2$.

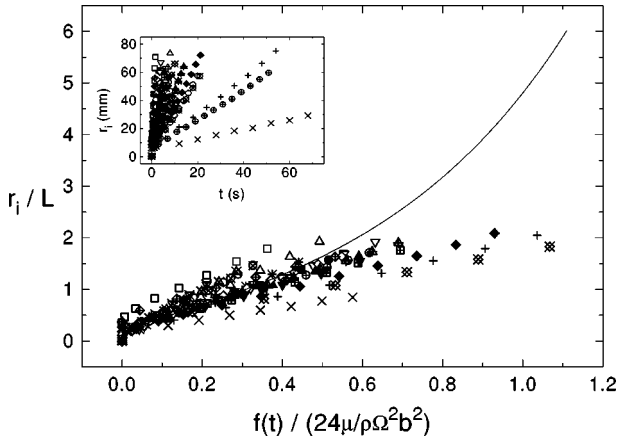

FIG. 6. Same as Fig. 4 but in a dry cell.

Figures 9, 10, and 11 present the capillary number obtained when the only parameter modified from one experiment to another is Ω_0 (angular velocity of the cell), $L(0)$ (initial radius of the drop), and b (gap thickness), respectively. The three plots show a power law dependence of Ca on the modified parameter. These results suggest an empirical relation between the capillary number Ca and a dimensionless combination of different experimental parameters, $S=\rho\Omega^2L^3/\sigma$. The relation reads

$$\mathrm{Ca}\sim\left(\frac{b}{L}\right)^2 S^{5/4}, \tag{16}$$

where we have rounded the exponents for convenience. When all the experimental data for the silicone oils obtained in dry conditions are represented in this form, Fig. 12 shows that they collapse remarkably into a single straight line for about three orders of magnitude in both Ca and the dimensionless group $(b/L)^2S^{5/4}$. To check the dependence on σ and ρ, we have also performed experiments with vaseline oil and scaled them in the way proposed. Figure 12 shows that both fluids scale with the same combination of parameters and the same proportionality constant.

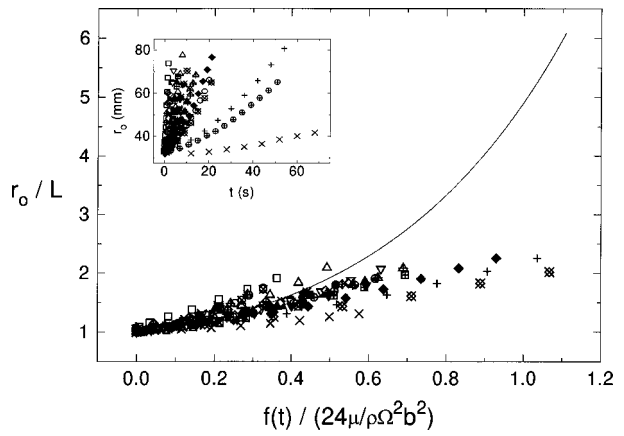

FIG. 7. Same as Fig. 5 but in a dry cell.

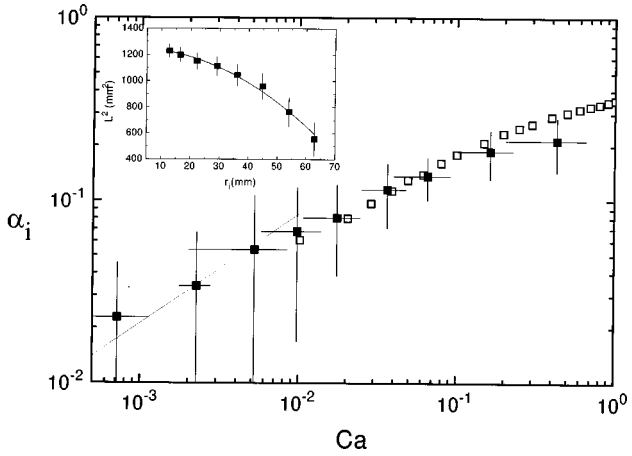

FIG. 8. Log–log plot of the relative thickness of the coating film left by the inner interface, α_i, as a function of capillary number Ca. The solid squares represent the values obtained in our experiments in dry conditions, from fits of L^2 against r_i (as the one shown in the inset). The open squares are numerical predictions of Reinelt, extracted from Fig. 3 of Ref. 20. The straight line is a power-law fit of the form $\alpha_i \sim \mathrm{Ca}^x$ with $x=2/3$, which corresponds to the prediction of Park and Homsy (Ref. 9) for low Ca ($\leqslant 10^{-3}$).

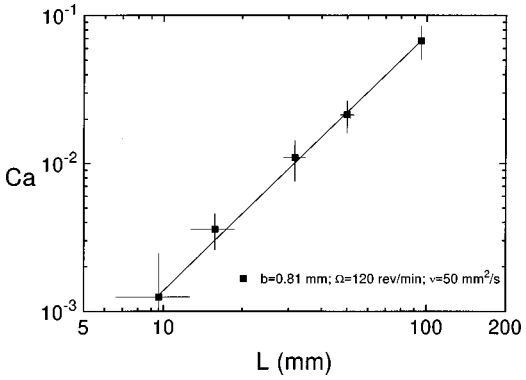

FIG. 10. Set of measurements of the capillary number as a function of initial radius of the drop in a dry cell. The line is a fit of the form $L^{1.72}$.

IV. DISCUSSION

Although our experiments have explored the same range of capillary and centrifugal forces in both prewet and dry conditions, the results show that the radial displacement of the annulus is very different in these two cases. The purpose of this section is to discuss how the wetting conditions at the leading interface modify the flow.

We discuss first the flow in prewet conditions. In this case our experimental results show that mass losses are negligible, except at the latest times. This means that the loss of fluid at the trailing interface (in the form of two coating films left behind this interface, one on each glass plate) is balanced by the fluid recovered from the plates at the leading interface. This being the case, the dynamic contact angles at r_i and r_o must be very similar (full wetting ensures that they will be close to zero). Hence, the contribution of capillary forces to the radial velocity due to the curvature of the interfaces in the vertical direction (perpendicular to the plates), which is given by $\sigma(\kappa_{\perp i}-\kappa_{\perp o}) \simeq (2\sigma/b)(\cos\theta_{Di}-\cos\theta_{Do})$, vanishes. This explains why the results in prewet conditions can be scaled without using the surface tension σ. This is no longer true in the long time limit, however, for which Figs. 4 and 5 already show deviations from the behavior predicted by Eq. (15); at large radii, mass losses are appreciable even in prewet conditions. It must be mentioned also that, similarly, experiments carried out in the extreme limit of small initial radii L and large Ω show the annulus to become progressively thinner, due to mass losses, until the meniscus breaks and only a fluid film remains on each plate.

The dry cell conditions modify the behavior of the leading (outer) interface for two main reasons. First, in a dry cell the annulus has no fluid income through this interface. As a result, L decreases appreciably with time, and the motion of the annulus becomes dependent on initial conditions—in the sense that a different velocity is measured for a drop of initial outer radius $L(0)$, for example, than for an annulus that has evolved up to an area $\pi L^2(0)$. The results shown in Fig. 10 confirm this observation. A gradual loss of fluid slows down the trailing interface (in comparison with its motion in conditions of mass conservation) as shown by Eq. (13). Opposite to this effect is the effect of the wetting films left by the trailing interface, which according to Eq. (8) increase the velocity of this interface. This last effect, however, is also present in prewet conditions, and seems to be of secondary importance. In particular, notice that the coating thickness α_i (which can be measured only in dry cell conditions) seems to

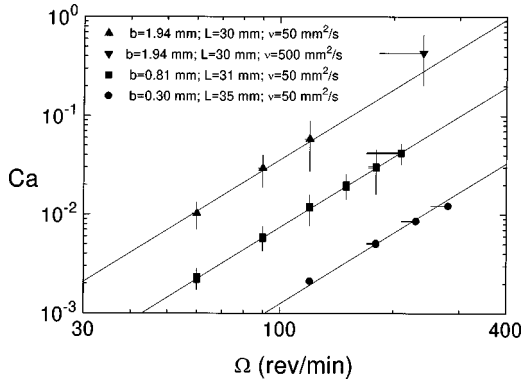

FIG. 9. Sets of measurements of the capillary number as a function of angular velocity in a dry cell. The lines are fits of the form $\Omega^{2.36}$.

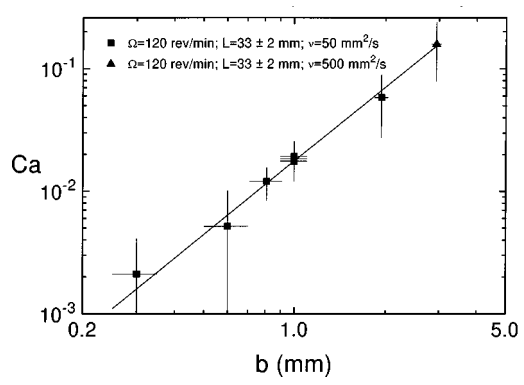

FIG. 11. Set of measurements of the capillary number as a function of gap thickness in a dry cell. The line is a fit of the form b^2.

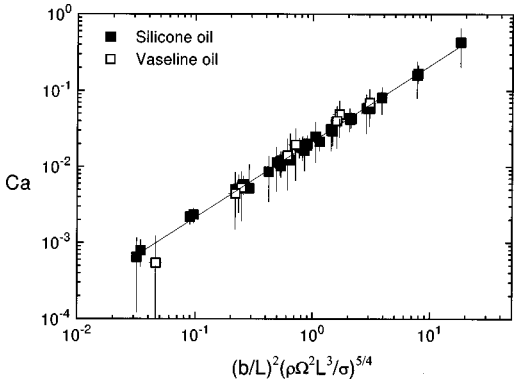

FIG. 12. Log–log plot of the capillary number Ca against $(b/L)^2S^{5/4}$, with $S=\rho\Omega^2L^3/\sigma$, measured in a dry cell in many different experimental conditions. The straight line is a fit of the form $\mathrm{Ca}=0.1(b/L)^2S^{5/4}$.

depend solely on Ca. The second and presumably most important reason is that the contact angle between the leading interface and the glass plates depends sensitively on the velocity of the flow. For small Ca the dynamic contact angle follows Tanner's law,[22] $\theta_D \sim \mathrm{Ca}^{1/3}$. As Ca increases, the dynamic contact angle increases correspondingly and may become larger than $\pi/2$, which represents an inverted meniscus.[13,17] Hoffman[17] in particular shows that the reversion of the meniscus is attained already at moderate Ca. In conclusion, the contact angles of the meniscus at the leading interface admit large variations, while at the trailing interface remain always close to zero (full wetting). It is for this reason that the difference in pressure jump between the two interfaces, in dry conditions, admits variations between 0 and $4\sigma/b$, which indeed have a large influence on the velocity of the annulus [Eq. (13)].

Once it is recognized that the role of capillary forces on the radial displacement of the annulus is negligible in prewet conditions, but may be very relevant in dry conditions, the need of introducing a new dimensionless number to scale the results in dry conditions seems natural. The number chosen, $S=\rho\Omega^2L^3/\sigma$, represents a balance between centrifugal and capillary forces. It appears naturally in several problems of interfaces subjected to centrifugal forces.[11,12,15]

Our results on α_i are consistent with the power-law dependence $\alpha_i \sim \mathrm{Ca}^x$ derived analytically for low Ca.[9,20] A comparison with Reinelt's numerical predictions included in Fig. 8 shows good agreement with our absolute values of thickness in the range of Ca where they overlap, particularly remarkable considering that the comparison does not make use of any adjustable parameter. The discrepancies at the largest Ca, which in any case are subject to large experimental uncertainties, may be due to the dispersion of the coating film under the influence of centrifugal forces.[15]

V. CONCLUSIONS

The radial displacement of a stable fluid annulus in a rotating Hele–Shaw cell is strongly influenced by the wetting conditions encountered by the advancing interfaces.

When the fluid front moves in a prewet cell, the amount of fluid in the annulus remains practically constant. In a wide range of experimental parameters, the flow is very well described by Eq. (15), which disregards capillary effects.

When the interface advances in dry plates, on the contrary, the flow is strongly influenced by the mass loss at the inner interface and by capillary effects at the outer interface. Instead of increasing with time, the velocity of the inner interface remains constant; this enables us to define a capillary number Ca characteristic of the flow. We have found experimentally that the two dimensionless numbers representative of the relevant forces in the problem, Ca and *S*, keep a relatively simple relation for a very wide range of experimental parameters and for two different fluids. This relation arises from an interplay between three effects; the formation of a coating film, which increases the velocity of the inner meniscus; the mass loss, which slows down the annulus; and the effects of capillary forces, whose influence depends on dynamic contact angles.

The relationship found between Ca and *S*, firmly supported experimentally, requires a theoretical explanation. It raises interesting questions about the role of dynamic contact angles on fluid flows in the Hele–Shaw approximation.

The thickness of the coating film left by the inner interface, α_i, is found to depend on Ca in a way consistent with previous theoretical and numerical predictions.

The phenomena studied in this work are relevant for the stability of the fluid annulus. The interfacial instabilities experienced by the rotating annulus will be the subject of a forthcoming paper.[19]

ACKNOWLEDGMENTS

The authors are indebted to L. Kramer and J. Casademunt for interesting suggestions. L.C. and J.S. are supported by the Dirección General de Enseñanza Superior (DGES, Spain). This work has received the financial support of the DGES (Spain) within Projects Nos. PB96-0378-C02-01 and PB97-0906, and has been developed in the framework of the *Training and Mobility of Researchers* program of the European Community (network project ERB 4061 PL95-1377).

APPENDIX: INFLUENCE OF THE INITIAL ACCELERATION OF THE ROTATING CELL

Equation (15) has been obtained in the assumption that the rotating cell achieves the preset velocity Ω_0 instantaneously. Actually, in our experimental setup there is a transient from $\Omega=0$ to the steady value Ω_0, which is well represented by the following dependence of Ω on *t*:

$$\Omega=\Omega_0[1-\exp(-\omega t)], \tag{A1}$$

where $\omega=1.2(300/\Omega_0)^{2.5}$, and both Ω and Ω_0 are given in rev/min. In general, for most experiments, the transient time is negligible. Nevertheless, there are a few experiments in which the transient time becomes comparable to the time of the experiment. In this case, we must integrate Eq. (14) between $t=0$ and t taking into account that $\Omega=\Omega(t)$,

$$\left[\left(\frac{r_i^2}{L^2}+1\right)\ln\left(\frac{r_i^2}{L^2}+1\right)-\frac{r_i^2}{L^2}\ln\frac{r_i^2}{L^2}\right]_{r_i(0)}^{r_i(t)}=\frac{b^2}{12\mu}\,\frac{1}{2}\,\rho\Omega_0^2 f(t). \tag{A2}$$

The function $f(t)$ stands for

$$f(t)\equiv\frac{1}{\Omega_0^2}\int_0^t\Omega^2(t)dt=\frac{1}{\omega}\left(\omega t-\frac{3}{2}-\frac{1}{2}e^{-2\omega t}+2e^{-\omega t}\right). \tag{A3}$$

It is not difficult to check that $f(t)\to t$ in the limit $\omega\to\infty$, i.e., when $\Omega=\Omega_0$.

Equation (A2) shows that all the temporal dependence of the moving interface is given by $f(t)$. Consequently, it is natural to represent the evolution of the interfaces as a function of $f(t)$, rather than as a function of t.

[1] P. G. Saffman and G. I. Taylor, ''The penetration of a fluid into a porous medium or Hele–Shaw cell containing a more viscous liquid,'' Proc. R. Soc. London, Ser. A **245**, 312 (1958).

[2] D. Bensimon, L. P. Kadanoff, S. Liang, B. J. Shraiman, and C. Tang, ''Viscous flows in two dimensions,'' Rev. Mod. Phys. **58**, 1 (1986).

[3] K. V. McCloud and J. V. Maher, ''Experimental perturbations to Saffman–Taylor flow,'' Phys. Rep. **260**, 139 (1995).

[4] P. Pelcé, *Dynamics of Curved Fronts* (Academic Press, New York, 1988).

[5] R. L. Chuoke, P. van Meurs, and C. van der Poel, ''The instability of slow, immiscible, viscous liquid–liquid displacements in permeable media,'' Trans. Am. Inst. Min. Metall. Pet. Eng. **216**, 188 (1959).

[6] T. Maxworthy, ''Experimental study of interface instability in a Hele–Shaw cell,'' Phys. Rev. A **39**, 5863 (1989).

[7] J. A. Miranda and M. Widom, ''Weakly nonlinear investigation of the Saffman–Taylor problem in a rectangular Hele–Shaw cell,'' Int. J. Mod. Phys. B **12**, 931 (1998).

[8] J. A. Miranda and M. Widom, ''Radial fingering in a Hele–Shaw cell: A weakly nonlinear analysis,'' Physica D **120**, 315 (1998).

[9] C. W. Park and G. M. Homsy, ''Two-phase displacements in Hele–Shaw cells: theory,'' J. Fluid Mech. **139**, 291 (1984).

[10] J. V. Maher, ''Development of viscous fingering patterns,'' Phys. Rev. Lett. **54**, 1498 (1985).

[11] L. W. Schwartz, ''Instability and fingering in a rotating Hele–Shaw cell or porous medium,'' Phys. Fluids A **1**, 167 (1989).

[12] Ll. Carrillo, F. X. Magdaleno, J. Casademunt, and J. Ortín, ''Experiments in a rotating Hele–Shaw cell,'' Phys. Rev. E **54**, 6260 (1996).

[13] G. E. P. Elliot and A. C. Riddiford, ''Dynamic contact angles. I. The effect of impressed motion,'' J. Colloid Interface Sci. **23**, 389 (1967).

[14] S. S. S. Cardoso and A. W. Woods, ''The formation of drops through viscous instability,'' J. Fluid Mech. **289**, 351 (1995).

[15] F. Melo, J. F. Joanny, and S. Fauve, ''Fingering instability of spinning drops,'' Phys. Rev. Lett. **63**, 1958 (1989).

[16] M. A. Spaid and G. M. Homsy, ''Stability of viscoelastic dynamic contact lines: An experimental study,'' Phys. Fluids **9**, 823 (1997).

[17] R. L. Hoffman, ''A study of the advancing interface. I. Interface shape in liquid–gas systems,'' J. Colloid Interface Sci. **50**, 228 (1975).

[18] E. B. Dussan, ''On the spreading of liquids on solid surfaces: static and dynamic contact lines,'' Annu. Rev. Fluid Mech. **11**, 371 (1979).

[19] Ll. Carrillo, J. Soriano, and J. Ortín (to be published).

[20] D. A. Reinelt, ''Interface conditions for two-phase displacement in Hele–Shaw cells,'' J. Fluid Mech. **183**, 219 (1987).

[21] E. Meiburg, ''Bubbles in a Hele–Shaw cell: Numerical simulation of three-dimensional effects,'' Phys. Fluids A **1**, 938 (1989), and references therein.

[22] L. H. Tanner, ''The spreading of silicone oil drops on horizontal surfaces,'' J. Phys. D **12**, 1473 (1979).